Polymer 50 (2009) 983–989

Contents lists available at ScienceDirect

Polymer

journal homepage: www.elsevier.com/locate/polymer

Mesostructured silica for the reinforcement and toughening of rubbery and glassy epoxy polymers

Jian Jiao [a,b], Xin Sun [a], Thomas J. Pinnavaia [a,*]

[a] Department of Chemistry, Michigan State University, East Lansing, MI 48824, USA
[b] Department of Applied Chemistry, Northwestern Polytechnic University, Xi'an, Shaanxi 710072, PR China

ARTICLE INFO

Article history:
Received 9 October 2008
Received in revised form
16 December 2008
Accepted 22 December 2008
Available online 30 December 2008

Keywords:
Epoxy composites
Mesostructured silica
Polymer reinforcement and toughening

ABSTRACT

Mesoporous forms of silica with wormhole framework structures prepared from tetraethylorthosilicate (denoted MSU-J-TEOS) or from sodium silicate (denoted MSU-J-SS) and an amine surfactant as the structure-directing porogen are highly effective reinforcing and toughening agents for rubbery and glassy epoxy polymers. The improvements in tensile strength and modulus provided by MSU-J silicas with a large average framework pore size (e.g., 5.9 and 21.3 nm) are superior to those provided by the corresponding silicas made from the same TEOS or SS precursors but with smaller framework pore sizes (e.g., 4.2 and 5.2 nm). The improved performance of the larger pore structures is realized even though the surface areas (~670 m^2/g) are substantially lower than the surface areas of the smaller pore analogs (812–1025 m^2/g), most likely, because of more efficient polymer impregnation of the particle mesopores. In comparison to the MSU-J-TEOS silica assembled from TEOS, MSU-J-SS silica made from SS exhibits a more uniform pore distribution and smaller particles. These latter textural features lead to improved tensile strength and modulus without compromising the strain-at-break for both rubbery and glassy epoxy polymers. The exceptional strength and toughness provided by MSU-J-SS silica in comparison to MSU-J-TEOS silica are correlated with the high degree of dispersion of the mesophase particles in the epoxy matrix for the more effective distribution of stress and the deflection of microcracks.

1. Introduction

Epoxy polymers are used extensively as adhesives, coatings and sealants. Due to their amorphous structure, these thermoset polymers generally exhibit relatively poor toughness in comparison to semi-crystalline thermoplastics. The incorporation of thermoplastics [1] or elastomers [2–4] into an epoxy matrix can be an effective way to improve toughness, but it can compromise strength or modulus. Functional fillers, such as organoclays [5,6] and related organosilica particles [7], also can improve the toughness of an epoxy resin, but the need for an organic surface modifier to achieve particle dispersion adds to the cost of such fillers. Silica nanoparticles with unmodified surfaces also are capable of providing improved epoxy strength, stiffness and toughness, but at the cost of lowering the glass transition temperature [8].

Ordered mesoporous silica particles with controllable mesopore sizes (2–50 nm), surface areas and ordered hexagonal, cubic, and wormhole framework structures can be assembled from organosilicon precursors (e.g. tetraethylorthosilicate, TEOS) [9–12] or purely inorganic reagents (e.g., sodium silicate and colloidal silica) [12–18]. These mesostructured forms of silica show considerable promise as reinforcing agents for several engineering polymer systems at relatively low particle loadings due in part to the high surface area and favorable interfacial interactions between the polymer and the silica surface [19–26]. The unique pore structures provide enough intraparticle space for the polymer to impregnate the particles and form a unique composite structure. For instance, the one-dimensional mesostructure represented by MCM-41 silica and the three-dimensional mesostructure of MCM-48 silica with pore sizes of ~3 nm have been studied as reinforcing agents for polyimide [19], poly((3-trimethoxysily) propyl methacrylate) [20], poly(vinyl acetate) [21], poly(methyl methacrylate) [22], Nylon 66 [23] and polypropylene [24]. Some of these composites exhibited improved tensile strength and tensile modulus as well as marginal improvements in toughness at specific loadings. In addition, the three-dimensional wormhole framework structure of MSU-J silica (5.3 nm pore size) [25] and the mesocellular foam structure of

* Corresponding author. Department of Chemistry, Michigan State University, 320 Chemistry Bldg, East Lansing, MI 48824, USA. Tel.: +1 517 432 1222; fax: +1 517 432 1225.
E-mail address: pinnavaia@chemistry.msu.edu (T.J. Pinnavaia).

0032-3861/$ – see front matter © 2008 Elsevier Ltd. All rights reserved.
doi:10.1016/j.polymer.2008.12.042

MSU-F silica (26.6 nm pore size) [26] have been shown to function as reinforcing and toughening agents in rubbery epoxy matrices at low loadings.

In an effort to better understand the factors that influence the mechanical properties of epoxy composites made from mesostructured forms of silica, we have initiated a study of the relationships between the tensile properties of the composites and the pore size and surface area of the silica. In the present study, we investigate the reinforcing properties of mesostructured silica with wormhole framework structures when dispersed at 2.0–10 wt% loadings in rubbery and glassy epoxy matrices. The silica mesostructures, denoted MSU-J silicas, were assembled from both an organosilica source (tetraethylorthosilicate, TEOS) and inorganic silica source (sodium silicate) in the presence of Jeffamine D2000, a commercially available α,ω-polyoxypropylene diamine surfactant, as the structure-directing porogen. Depending on the reaction conditions used to assemble the silica mesophases, the average framework pore size could be increased from ~4 nm to ~21 nm and the surface areas could be varied over a wide range from 670 to 1025 m^2/g.

2. Experimental section

2.1. Materials

The commercially available diglycidyl ethers of bisphenol A (DGEBA), namely Epon 828 and Epon 826 (Hexion Specialty Chemicals, Inc.), were used in forming rubbery and glassy epoxy composites, respectively. The α,ω-polyoxypropylene diamine $H_2NCH(CH_3)CH_2[OCH_2CH(CH_3)]_xNH_2$ (Huntsman Chemicals Jeffamine D2000 with $x = 33$ and D230 with $x = 2.6$) was used as the curing agent for the rubbery and glassy systems, respectively. Jeffamine D2000 also was used as a mesostructure-directing agent in the synthesis of MSU-J silicas. Tetraethylorthosilicate (TEOS) and sodium silicate were purchased from Aldrich Chemical Co. and used as the silica precursors to assemble mesostructured silica.

2.2. Assembly of mesostructured silica MSU-J-TEOS and MSU-J-SS

In a typical synthesis of mesostructured silica from TEOS [17], the Jeffamine D2000 surfactant was dissolved in ethanol and then the desired amount of water was added under stirring. TEOS was added to the surfactant solution under vigorous stirring at ambient temperature. The resulting mixture was allowed to age in a heated water bath at the desired synthesis temperature for 20 h with shaking. The surfactant was then removed from the washed and air-dried solid by calcination at 600 °C for 4 h in air. The surfactant-free product made from TEOS was denoted MSU-J-TEOS-*T* (where *T* indicates the assembly temperature). The molar composition of the reaction mixture was $TEOS:D2000:H_2O:EtOH = 1:0.125:220:17$.

In a typical synthesis of mesostructured MSU-J silica from sodium silicate [17], the Jeffamine D2000 surfactant was mixed with an amount of aqueous HCl solution equivalent to the hydroxide content of the sodium silicate solution. The silica resource was added to the porogen solution under vigorous stirring at ambient temperature, and the mixture was allowed to age at the desired assembly temperature for 20 h. The surfactant-intercalated mesostructured product was recovered by filtration and dried in air at 80 °C. A surfactant-free analogue of the mesostructure, denoted MSU-J-SS-*T* (where *T* indicates the assembly temperature), was obtained by calcination of as-made MSU-J-SS at 600 °C for 4 h. The molar composition for the formation of MSU-J-SS was $SiO_2:NaOH:D2000:HCl:H_2O = 1.0:0.83:0.125:0.83:230$.

Table 1
Textural properties of MSU-J-TEOS silica and MSU-J-SS silica.

Sample	d_{100} (nm)	Average pore diameter (nm)	V_{tot} (cm^3/g)	S_{BET} (m^2/g)	Wall thickness[a] (nm)
MSU-J-TEOS-25 °C	6.5	4.2	1.76	1025	2.3
MSU-J-TEOS-65 °C	[b]	21	2.25	670	–
MSU-J-SS-25 °C	6.0	5.2	1.34	812	0.8
MSU-J-SS-65 °C	7.0	5.9	1.66	674	1.1

[a] Wall thickness was determined by subtracting the BJH pore diameter from the pore–pore correlation distance from XRD.
[b] The d_{001} reflection for this sample was too broad to observe the diffraction maximum.

2.3. Preparation of epoxy composites

Rubbery and glassy composites were prepared by first adding a desired amount of mesostructured silica into the epoxy resin and mixed at 50 °C for 10 min. The amount of amine curing agent needed to achieve an overall NH:epoxide stoichiometry of 1:1 was added to the mixture at 50 °C for another 10 min. The resulting suspensions were degassed under vacuum and transferred to an aluminum mold. Pre-curing of the composites was carried out under nitrogen flow at 75 °C for 3 h, followed by an additional 3 h curing at 155 °C to complete the cross-linking reaction.

2.4. Characterization methods

N_2 adsorption–desorption isotherms were obtained at −196 °C on a Micromeritics Tristar 3000 sorptometer. Calcined MSU-J silicas were outgassed at 150 °C and 10^{-6} Torr for a minimum of 12 h prior to analysis. BET surface areas were calculated from the linear part of the BET plot according to IUPAC recommendations. The Barrett–Joyner–Halenda (BJH) method was used to determine the pore size distribution from the adsorption branch of the isotherms.

X-ray diffraction (XRD) patterns were obtained on a Rigaku Rotaflex 200B diffractometer equipped with Cu K_α X-ray radiation and a curved crystal graphite monochromator operating at 45 kV and 100 mA.

Transmission electron microscopy (TEM) images were taken on a JEOL 2200FS microscope with field emission electron source and an accelerating voltage of 200 keV. Sample grids of mesoporous silica were prepared by sonicating the powdered sample in ethanol for 10 min and then evaporating 2 drops of the resulting suspension onto a holey carbon-coated film supported on 300 mesh copper

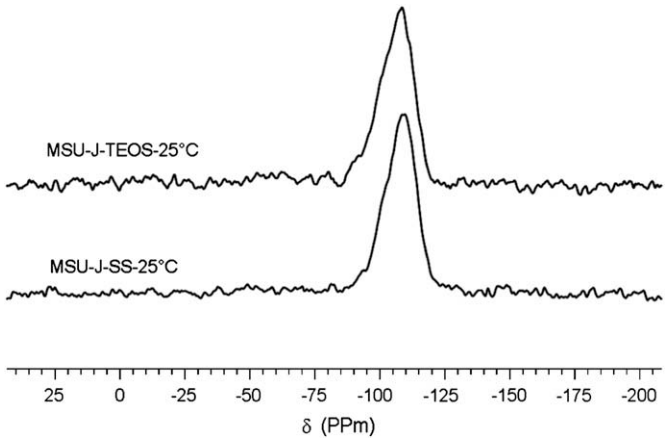

Fig. 1. ^{29}Si Mass NMR spectra for calcined forms (600 °C) of mesostructured silicas prepared from TEOS and sodium silicate at 25 °C.

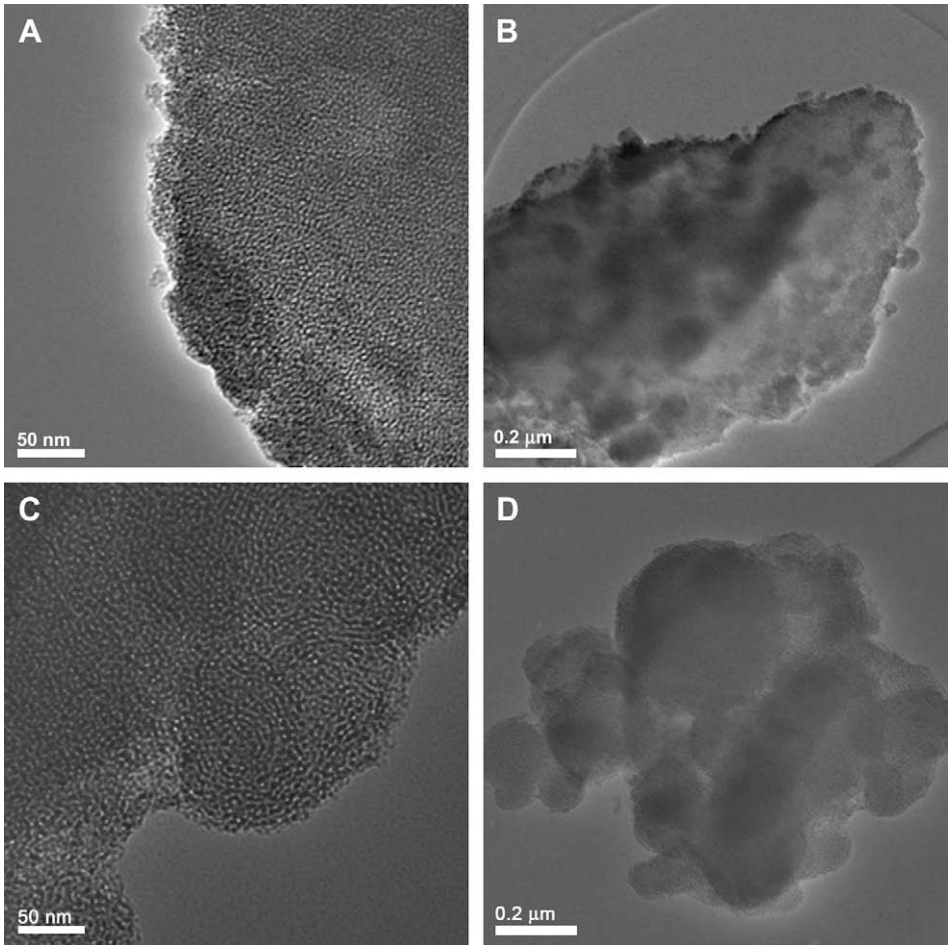

Fig. 2. Representative TEM image of calcined forms of (A and B) MSU-J-TEOS and (C and D) MSU-J-SS silica mesophases.

grids. Thin film specimens of glassy composites were prepared for TEM analysis using a microtome.

Scanning electron microscopy (SEM) samples were osmium coated for 4 min at a coating rate of 7 nm/min. Imaging was done at an accelerating voltage of 15 kV on a JEOL JSM-6400 V instrument.

^{29}Si MAS NMR spectra were obtained at 79 MHz on a Varian VXR-400S solid-state NMR spectrometer equipped with a magic angle-spinning probe. Sample was spun at 4 kHz for each measurement. The pulse delay for ^{29}Si MAS NMR was 400 s, and chemical shifts were referenced to talc.

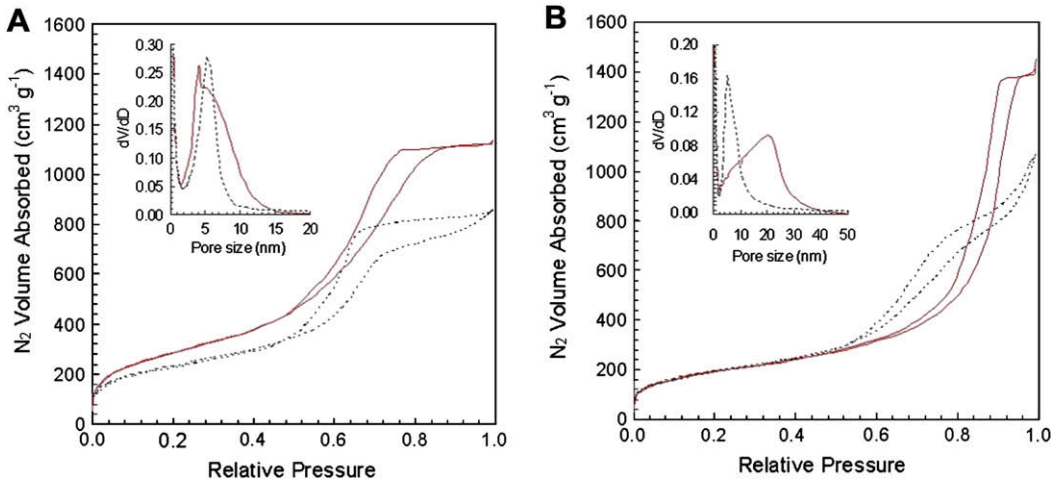

Fig. 3. N_2 adsorption–desorption isotherms of MSU-J-SS (– – –) silica and MSU-J-TEOS silica (——) with wormhole framework structures synthesized at (A) 25 °C and (B) 65 °C and calcined at 600 °C for 4 h. The insets provide BJH framework pore size distributions determined from the adsorption branches of the N_2 isotherms.

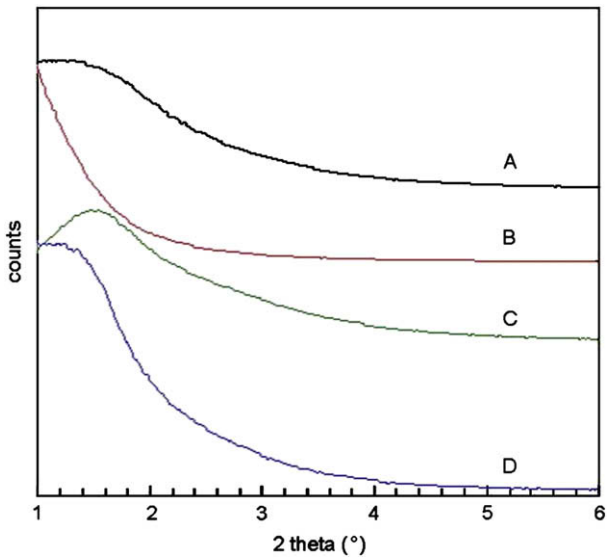

Fig. 4. XRD patterns of MSU-J-TEOS silica assembled from TEOS at (A) 25 °C and (B) 65 °C, and MSU-J-SS assembled from sodium silicate at (C) 25 °C and (D) 65 °C in the presence of Jeffamine D2000 as a structure director. The samples were calcined at 600 °C for 4 h.

The determination of tensile strength, tensile modulus and strain-at-break was performed at ambient temperature according to ASTM method D638 using an SFM-20 United Testing System. The dog-bone shaped specimens used in the tensile testing were 28 mm long in the narrow region, 2–3 mm thick, and 3 mm wide along the center of the casting for rubbery epoxy resin. The cross head speed was 10 mm/min for the rubbery epoxy resin specimens and 0.5 mm/min for glassy epoxy specimens. At least four specimens were tested to obtain the effective average value of tensile properties.

3. Results

3.1. Textural properties of mesostructured MSU-J-TEOS and MSU-J-SS silicas

Mesoporous silicas with wormhole framework structures (denoted MSU-J-TEOS-*T* and MSU-J-SS-*T*, where *T* indicates the assembly temperature) and a fundamental particle size of a few hundred nanometers [17] were assembled from TEOS and sodium silicate (SS) as the silica precursors and Jeffamine D2000 as the porogen at assembly temperatures of 25 °C and 65 °C. As shown in Table 1, the textural properties of the resulting mesostructures, as determined by nitrogen adsorption methods (discussed further below), were dependent on the nature of the silica source and the assembly temperature.

The framework cross-linking of MSU-J-SS-25 °C and MSU-J-TEOS-25 °C was characterized by ^{29}Si MAS NMR spectroscopy. As shown in Fig. 1 a strong Si(Q^4) signal and an unresolved lower field Si(Q^3) shoulder are observed for both silicas. This means that MSU-J-TEOS and MSU-J-SS exhibit hierarchical structures with equivalent Si–O–Si framework cross-linking.

As shown by the TEM images in Fig. 2A and B, the presence of mesoporous wormhole framework is verified for the mesostructured silicas, regardless of the silica precursor used in the assembling process. However, the particle morphology and textural properties differ depending on the silica source. MSU-J-TEOS assembled from TEOS at 25 °C exhibits micrometer to sub-micrometer aggregates of fundamental spherical particles of 10–100 nm in diameter, whereas the sub-micrometer aggregates of MSU-J-SS made under the same conditions from sodium silicate contain fundamental particles of larger diameter (≥100 nm). Also, the framework pore size distributions shown in the insets to the nitrogen isotherms of Fig. 3 are substantially broader for the MSU-J-TEOS derivatives than those for the MSU-J-SS analogs. Thus, although the average pore size for the mesostructures made at 25 °C is similar (cf., Table 1) the MSU-J-TEOS silica contains a larger fraction of pores greater than 6 nm in diameter. Also, the pore size distribution for MSU-J-SS silica shows little dependence on assembly temperature, whereas the pore distribution for MSU-J-TEOS broadens and the average pore size increases from 4.2 to 21 nm upon increasing the assembly temperature from 25 to 65 °C.

In accord with the wormhole framework structures revealed in the TEM images of the mesophases (cf., Fig. 2A and C), all of the products with the exception of MSU-J-TEOS-65 °C exhibit a low angle diffraction peak (see Fig. 4) corresponding to the pore-to-pore correlation distance of the framework. The absence of a diffraction peak for MSU-J-TEOS-65 °C most likely is a consequence of the very broad pore size distribution which broadens the diffraction peak to the point where it is not observable above background. Despite the differences in the framework pore sizes

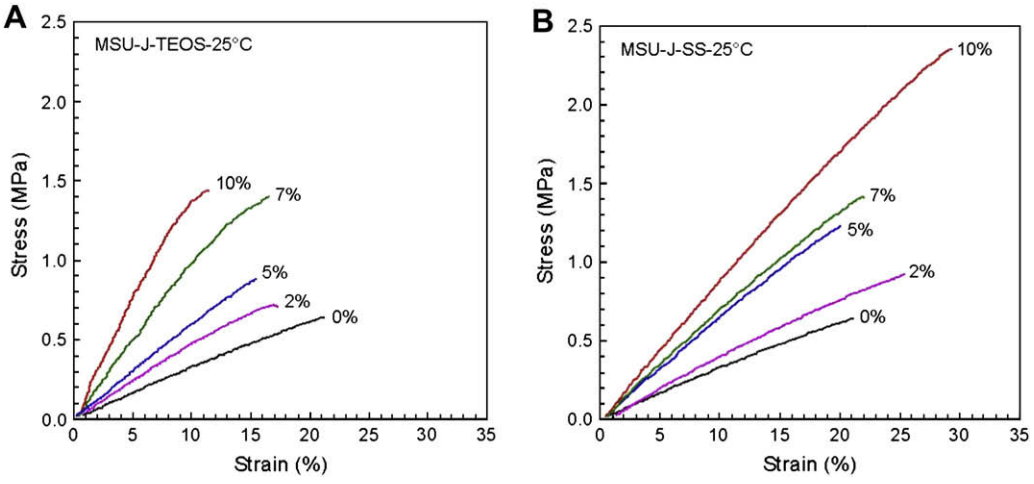

Fig. 5. Stress–strain curves for rubbery epoxy resin mesocomposites containing 0–10 wt% loadings of (A) MSU-J-TEOS-25 °C and (B) MSU-J-SS-25 °C.

Table 2
Tensile properties of rubbery epoxy mesocomposites.

Mesoporous silica	Silica loading (wt%)	Tensile strength (MPa)	Tensile modulus (MPa)	Strain-at-break (%)
Pristine epoxy	0	0.60	2.96	21.1
MSU-J-TEOS-25 °C (4.2 nm)	2	0.70	4.85	17.4
	5	0.87	6.79	16.0
	7	1.30	9.78	16.3
	10	1.42	14.6	11.6
MSU-J-TEOS-65 °C (21 nm)	2	0.82	4.77	20.0
	5	1.01	9.40	15.1
	7	1.30	10.0	13.1
	10	1.53	14.7	12.4
MSU-J-SS-25 °C (5.2 nm)	2	0.86	4.13	24.1
	5	1.19	7.03	20.7
	7	1.39	7.68	23.0
	10	2.06	9.56	24.1
MSU-J-SS-65 °C (5.9 nm)	2	1.36	4.93	31.2
	5	1.67	7.34	25.7
	7	1.98	8.56	25.7
	10	2.83	12.2	27.4

and pore distributions, all four forms of mesoporous silica exhibit large surface area in the range 670–1025 m^2/g (cf., Table 1).

3.2. Mechanical properties of rubbery mesoporous silica–epoxy composites

The average pore sizes of the silica mesophases are sufficiently large to allow both the epoxy resin and the curing agent to readily penetrate the internal space of mesostructured silica and form composite particles with a unique structure and composition. Direct evidence for polymer intercalation of the framework mesopores of MSU-J was obtained by filling the pores with an equivalent volume of liquid Jeffamine D-2000 and epoxy resin by incipient wetness methods, curing the mixture, and then determining the intensity of the *001* X-ray reflection in comparison to the unfilled silica mesophase. As expected for the contrast matching [27]

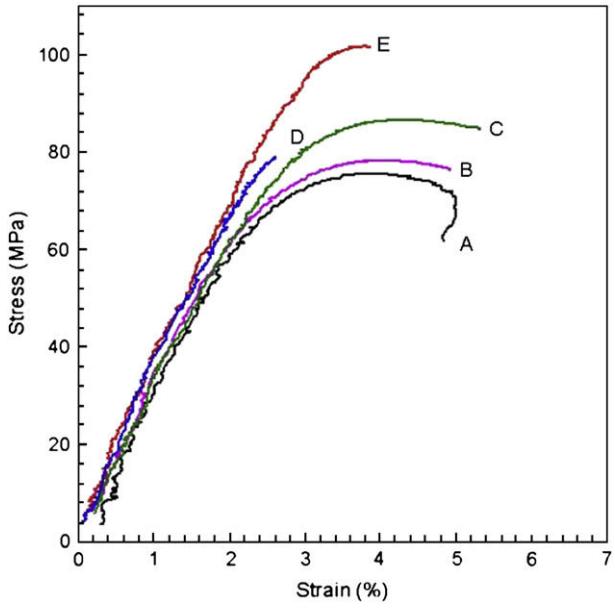

Fig. 6. Stress–strain curves for (A) a pristine glassy epoxy and 5 wt% composites reinforced by: (B) MSU-J-SS-25 °C, (C) MSU-J-SS-65 °C, (D) MSU-J-TEOS-25 °C and (E) MSU-J-TEOS-65 °C silicas.

Table 3
Tensile properties of glassy epoxy mesocomposites.

Mesoporous silica	Silica loading (wt%)	Strength (MPa)	Modulus (GPa)	Strain-at-break (%)	Yield strength (MPa)	Yield strain (%)
Pristine epoxy	0.0	75.8	3.00	4.29	75.8	3.81
MSU-J-TEOS-25 °C (4.2 nm)	5.0	79.3	3.52	2.70	–	–
MSU-J-TEOS-65 °C (21 nm)	5.0	89.6	3.94	3.62	–	–
MSU-J-SS-25 °C (5.2 nm)	5.0	80.9	3.30	4.48	80.2	4.00
MSU-J-SS-65 °C (5.9 nm)	5.0	87.0	3.25	5.18	86.9	4.35

provided by the intercalated polymer, a dramatic reduction in the intensity of the *001* X-ray reflection was observed for the composite relative to the intensity of this reflection for the pristine silica.

Owing to the large surface area and the more or less uniform pore size distribution of the silica mesophases, we anticipated a substantial improvement in the tensile properties of the composite. As shown by the representative stress–strain curves in Fig. 5, the tensile properties of the polymer indeed were improved through the dispersion of both MSU-J-TEOS and MSU-J-SS in the rubbery matrix made from epoxy resin Epon 828 and Jeffamine D2000 as the curing agent.

Table 2 summarizes the changes in strength, modulus, and elongation-at-break for the rubbery composites with increasing particle loading over the range 0–10 wt%. For both MSU-J-SS and MSU-J-TEOS, the larger pore derivatives assembled at 65 °C provide somewhat better reinforcement than their smaller pore analogs made at 25 °C. Regardless of the average pore size, however, the composites prepared from MSU-J-SS exhibit better tensile strength and strain-at-break (but a lower tensile modulus) in comparison to the composites prepared from MSU-J-TEOS. These improvements in tensile properties make MSU-J-SS a better toughening agent than MSU-J-TEOS.

3.3. Mechanical properties of glassy epoxy–mesoporous silica composites

Typical stress–strain curves are shown in Fig. 6 for glassy epoxy–mesoporous silica composites prepared from Epon 826 resin, Jeffamine D230 curing agent and 5 wt% mesoporous silica as the reinforcing agent. The tensile properties of the corresponding composites are summarized in Table 3.

As in the case of the rubbery composites, the larger pore mesophases provide somewhat better reinforcement at 5 wt% loading, than the corresponding smaller pore analogs in comparison to the pristine glassy epoxy. Regardless of the pore size, better strength and modulus are achieved with MSU-J-TEOS than with MSU-J-SS silica. Although composites made with MSU-J-SS show yield behavior, this mesophase provides superior elongation-at-break. Thus, MSU-J-SS silica is the better toughening agent for a glassy epoxy, as well as for a rubbery epoxy.

4. Discussion

The wormhole framework structures of MSU-J-TEOS and MSU-J-SS silicas are formed using the same α,ω-polyoxypropylene diamine porogen (Jeffamine D2000) as the structure-directing template. However, the former derivative is assembled from TEOS in an ethanol–water reaction medium, whereas the latter is made from aqueous sodium silicate. Although ^{29}Si NMR indicates the same degree of framework cross-linking for the wormhole structures, differences in the silicon source and the reaction media can lead to differences in the micellular properties of the surfactant porogen and consequently to differences in the textural properties of the templated mesophase [9,10,13,28,29]. For both mesophases, an

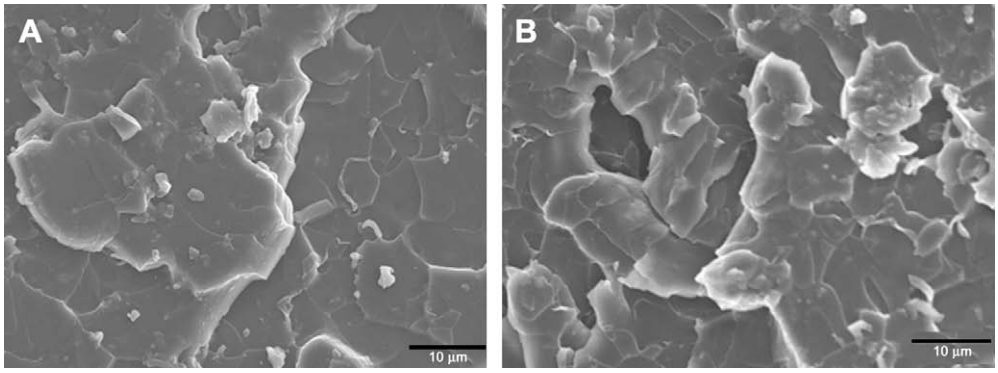

Fig. 7. SEM images of the tensile fracture surfaces of glassy epoxy mesocomposites containing 5 wt% loadings of (A) MSU-J-TEOS-25 °C silica and (B) MSU-J-SS-25 °C silica.

increase in the assembly temperature from 25 to 65 °C results in an increase in the average framework pore size at the expense of the framework surface area. However, the pore size and surface area for MSU-J-TEOS silica are far more sensitive to a change in assembly temperature in comparison to MSU-J-SS silica. For example, the average framework pore size of MSU-J-TEOS increases from 4.2 to 21 nm while the surface area decreases from 1025 to 670 m^2/g when the assembly temperature is increased from 25 to 65 °C. For the same change in assembly temperature, the average pore size of MSU-J-SS silica increases from 5.2 to only 5.9 nm while the surface area decreases from 812 to 674 m^2/g (cf., Table 1).

MSU-J-TEOS and MSU-J-SS silicas provide substantial improvements in the tensile properties of rubbery and glassy epoxy matrices at loading levels in the range 2.0–10 wt% (cf., Tables 2 and 3). Increasing the pore size of either silica mesophase (from 4.2 to 21 nm for MSU-J-TEOS or from 5.2 to 5.9 nm in the case of MSU-J-SS), along with a corresponding increase in the framework pore volume, generally results in an increase in strength, modulus and elongation-at-break, despite the loss of 17–35% of the framework surface area accompanying pore expansion. This suggests that the improvements in tensile properties depend more importantly on the amount of polymer filling the framework mesopores and the degree to which the pores are occupied by polymer than on the amount of surface area available for interfacial interactions between the polymer and the silica pore walls.

The silicon reagent and reaction medium used to assemble the mesoporous wormhole framework also have a significant influence on the reinforcement properties of the silica mesophase. For instance, for a rubbery epoxy matrix, a 10 wt% loading of MSU-J-TEOS silica with a 21 nm pore size increases the tensile strength and modulus 2.6- and 5.00-fold, respectively, but *decreases* the elongation-at-break by 30%. The same loading of MSU-J-SS silica with a 5.9 nm pore size increases the tensile strength and modulus by 4.7- and 4.1-fold, respectively, while *increasing* the elongation-at-break by 30%. Thus, the superior strength and elongation-at-break provided by MSU-J-SS silica make it a better toughening agent for a rubbery epoxy matrix. Although organoclays are capable of providing even larger 5- to 8-fold improvements in the tensile strength modulus of a rubbery epoxy matrix at a comparable loading, they provide no improvement in toughness [30].

The MSU-J-SS mesophase also is a superior toughening agent for a glassy epoxy matrix. For instance, at a loading of 5 wt% MSU-J-SS with a 5.9 nm pore size, the tensile strength and modulus of the glassy matrix are increased 14% and 8%, respectively, and the elongation at break is increased by an unprecedented 93%. Although MSU-J-TEOS at the same loading provides better reinforcement in terms of increased strength (+17%) and modulus (+30%), the elongation-at-break is significantly compromised (−37%). To our knowledge, the toughening effect of MSU-J-SS silica on a glassy epoxy matrix has not been equaled by any other mesoporous form of silica or organoclay filler.

The toughness and strength of epoxy–mesoporous silica composites depend on the strength of the interface between the rigid particles and the epoxy matrix and the micro-crack mechanism [31,32]. The toughening effect realized with mesoporous MSU-J-SS silica most likely arises due to crack deflection occurring when the crack front encounters the reinforcing particles and passes between the silica–polymer interface and forming micro-cracks

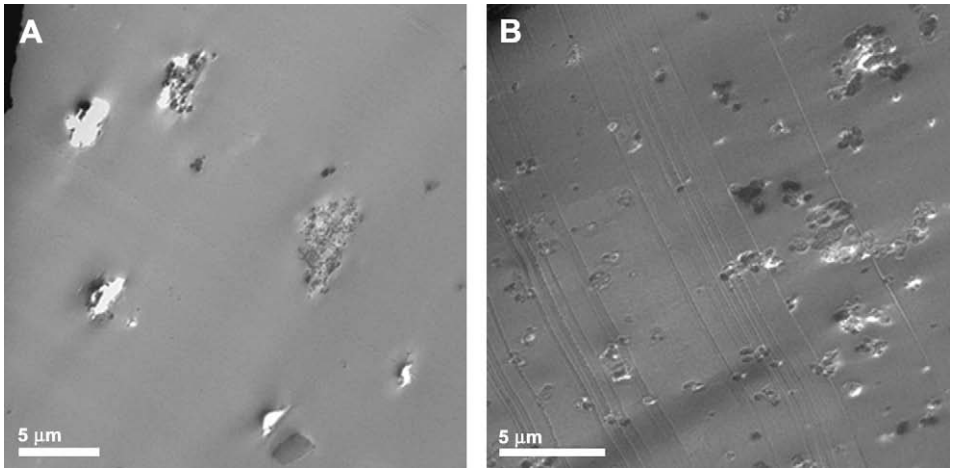

Fig. 8. Thin section TEM images of glassy epoxy mesocomposites containing 5 wt% loadings of (A) MSU-J-TEOS-25 °C silica and (B) MSU-J-SS-25 °C silica.

that release the fracture energy [33,34]. The mesoporosity associated with the reinforcing particle might facilitate microcrack formation within the particle itself, though evidence in support of intraparticle microcracking is lacking. In any case, the presence of mesoporosity alone cannot explain the toughening effect provided by MSU-J-TEOS-65 °C silica. MSU-J-SS-65 °C possesses substantially more mesopore volume than MSU-J-TEOS-65 °C (cf., Table 1), yet this mesophase is a comparatively poor toughening agent.

Fig. 7 provides SEM images of the fracture surfaces of the glassy epoxy–mesoporous silica composites prepared from MSU-J-TEOS and MSU-J-SS silicas. The composite prepared from MSU-J-SS shows a substantially rougher fracture surfaces in comparison to the fracture surfaces for the composite made from MSU-J-TEOS. The difference in fracture surface roughness correlates with the difference in particle dispersion. As shown by the SEM images of thin-sectioned specimens in Fig. 8, MSU-J-SS aggregates are smaller and much more homogenously dispersed in the epoxy matrix in comparison to MSU-J-TEOS. Thus, the smaller, well dispersed particles of mesoporous MSU-J-SS particles promote more crack deflections and smaller fracture domains. The more efficient deflection of cracks, which is facilitated by a combination of intrinsic particle mesoporosity and a uniform dispersion of small particle aggregates in the polymer matrix, leads to the superior toughening properties of MSU-J-SS silica.

5. Conclusions

Mesostructured forms of silica are effective reinforcement agents for both rubbery and glassy epoxy polymers. However, not all mesostructured forms of silica are equally effective in providing reinforcement benefits. For mesostructures assemble from identical reagents but different assembly temperatures, the derivatives with the largest framework pores provide the best reinforcement benefits, even though the increase in pore size occurs at the expense of interfacial surface area. Also, the reinforcement properties of the mesophases depend importantly on the particle size and dispersion of the particles in the polymer matrix. Uniformly dispersed sub-micrometer particles in combination with large framework pores facilitate crack deflection and provide, in addition to improved strength and modulus, unprecedented toughness even for glassy epoxy polymers. Moreover, these benefits are realized at low loadings ($\leq$10 wt%) and without the need for organic surface modifiers to achieve particle dispersion.

Acknowledgment

The support of this research by the National Aeronautics and Space Administration is gratefully acknowledged. J.J. acknowledges the support of China Scholarship Council for a State Fund Scholarship.

References

[1] Kishi H, Uesawa K, Matsuda S, Murakami A. J Adhes Sci Technol 2005; 19(15):1277–90.
[2] Harani H, Fellahi S, Bakar M. J Appl Polym Sci 1999;71(1):29–38.
[3] Oochi M, Kimura K, Motobe H. J Adhes Sci Technol 1994;8(3):223–33.
[4] Franco M, Mondragon I, Bucknall CB. J Appl Polym Sci 1999;72(3):427–34.
[5] Becker O, Varley R, Simon G. Polymer 2002;43(16):4365–73.
[6] Lan T, Pinnavaia TJ. Chem Mater 1994;6(12):2216–9.
[7] Zhang XH, Xu WJ, Xia XN, Zhang ZH, Yu RQ. Mater Lett 2006;60(28):3319–23.
[8] Rosso P, Ye L, Friedrich K, Sprenger S. J Appl Polym Sci 2006;101(2):1235–6.
[9] Pauly TR, Pinnavaia TJ. Chem Mater 2001;13(3):987–93.
[10] Kipkemboi P, Fogden A, Alfredsson V, Flodstrom K. Langmuir 2001; 17(17):5398–402.
[11] Zhang W, Pauly TR, Pinnavaia TJ. Chem Mater 1997;9(11):2491–8.
[12] Boissiere C, Larbot A, Prouzet E. Chem Mater 2000;12(7):1937–40.
[13] Berggren A, Palmqvist AEC, Holmberg K. Soft Matter 2005;1(3):219–26.
[14] Kim SS, Pauly TR, Pinnavaia TJ. Chem Commun 2000;10:835–6.
[15] Kim SS, Karkamkar A, Pinnavaia TJ, Kruk M, Jaroniec M. J Phys Chem 2001;105(32):7663–70.
[16] Kim SS, Pauly TR, Pinnavaia TJ. Chem Commun 2000;17:1661–2.
[17] Park I, Wang Z, Pinnavaia TJ. Chem Mater 2005;17(2):383–6.
[18] Pauly TR, Petkov V, Liu Y, Billinge SJL, Pinnavaia TJ. J Am Chem Soc 2002;124(1):97–103.
[19] Lin J, Wang X. Polymer 2007;48(1):318–29.
[20] Ji X, Hampsey JE, Hu Q, He J, Yang Z, Lu Y. Chem Mater 2003;15(19):3656–62.
[21] He J, Shen YB, Yang J, Evans DG, Duan X. Chem Mater 2003; 15(20):3894–902.
[22] Run MT, Wu SZ, Zhang DY, Wu G. Mater Chem Phys 2007;105(2–3):341–7.
[23] Kojima Y, Matsuoka T, Takahashi H. J Appl Polym Sci 1999;74(13):3254–8.
[24] Wang N, Li TM, Zhang JS. Mater Lett 2005;59(21):2685–8.
[25] Park I, Peng HG, Gidley DW, Xue SQ, Pinnavaia TJ. Chem Mater 2006; 18(3):650–6.
[26] Park I, Pinnavaia TJ. Adv Funct Mater 2007;17(15):2835–41.
[27] Kleitz F, Schmidt W, Schuth F. Microporous Mesoporous Mater 2003; 65(1):1–29.
[28] Blin JL, Leonard A, Su BL. Chem Mater 2001;13(10):3542–53.
[29] Renzo DF, Testa F, Chen JD, Cambon H, Galarneau A, Plee D, et al. Microporous Mesoporous Mater 1999;28(3):437–46.
[30] Shi H, Lan T, Pinnavaia TJ. Chem Mater 1996;8(8):1584–7.
[31] Tjong SC. Mater Sci Eng R Rep 2006;53(3–4):73–197.
[32] Zhao Q, Hoa SV. J Compos Mater 2007;41(2):201–19.
[33] Kinloch AJ, Taylor AC. J Mater Sci 2002;37(3):433–60.
[34] Johnsen BB, Kinloch AJ, Mohammed RD, Taylor AC, Sprenger S. Polymer 2007;48(2):530–41.